# A Search for Primary Cosmic Gamma-Radiation. II. Low Energy Radiation above and within the Atmosphere

GILBERT J. PERLOW AND CHARLES W. KISSINGER*
*U. S. Naval Research Laboratory, Washington, D. C.*
(Received July 23, 1951)

Measurements are reported on the intensity of gamma-rays in the energy range 0.1 to 15 Mev, made in a series of rocket flights. The gamma-radiation was detected by anticoincidence in a bundle of Geiger counters. Registration of coincidences permitted a measurement of the intensity of charged particles, with the same geometry. The two quantities displayed a simultaneous maximum during flight, the counting rate of charged particles being ten times that of $\gamma$-rays at the maximum. A diurnal effect was looked for and not found. A theoretical treatment is given of the origin of the $\gamma$-radiation at the maximum. It is shown to be accountable for by bremsstrahlung of the electronic component and subsequent multiple Compton scattering. An estimate is given of the radiation due to annihilation of positrons followed by Compton scattering. This is shown to be only a few percent of the bremsstrahlung effect.

After all corrections are applied a weak residual $\gamma$-radiation is found above the atmosphere. Arguments are given for identifying this as an albedo. Two types of albedo are considered, the first and more important is associated with back-scattering and is not calculated, while the second is due to the curvature of the earth. A calculation shows the latter to give 25 percent of the observed counting rate at 82 km.

In conjunction with the conclusions of paper I of this series and with other evidence at higher energies, it is concluded that primary cosmic gamma-radiation contributes at most a very small fraction to the incoming cosmic-ray energy flux.

## I. INTRODUCTION

IN a previous paper[1] we reported on a rocket measurement of the primary cosmic gamma-ray energy flow into the atmosphere for the energy range 3.4 to 90 Mev. Our measurement indicated a possible energy flux, in the range investigated, of one part in 1300 of the total incoming energy given by the ionization integrals of Millikan and co-workers. The difficulty of assessing all corrections made a null result admissible however. It was pointed out that gamma-rays in the Bev range apparently are ruled out by other evidence. The experiment reported here is an investigation of lower energies, with some overlapping of the previous work. The detector was sensitive to gamma-rays from 0.1 Mev to 15 Mev with maximum efficiency at about 7 Mev. It was felt that if a null or very small flux were obtained, one would be justified in assuming a similar result for the spectral regions as yet unexplored.[2] This conclusion would have certain cosmological implications.

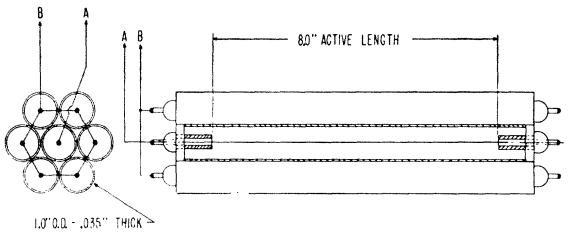


FIG. 1. The apparatus. Anticoincidences $A$–$B$ detected low energy $\gamma$-rays in $A$. Coincidences $AB$ detected charged particles in $A$.

The present experiment was performed three times, first in the V-2 rocket of the previous paper, and later in two Aerobee rockets. One of the latter flights was made at night in order to detect any diurnal effect. The flights were made at White Sands, New Mexico, geomagnetic latitude 41°. Additional measurements with a scaled-down version of the detector were made by Bergstralh and Schroeder[3] using Skyhook balloons at Camp Ripley, Minnesota. They looked for a diurnal effect and found none as large as their statistical probable error (about 3 percent).

Section II describes the experimental method and the results. In Sec. III a theoretical treatment is given of the radiation encountered in the atmospheric portion of the flight. Section IV treats the radiation observed above the atmosphere. The analysis shows that the atmospheric radiation can reasonably be accounted for by bremsstrahlung and multiple Compton scattering in the electronic component, and that some of the radiation found above the atmosphere, possibly all of it, is secondary to processes lower down.

## II. EXPERIMENTAL METHOD

Figure 1 illustrates the apparatus. It consisted of a tightly packed bundle of seven Geiger counters, each having 0.035-in. Cu wall thickness and a nominal active length of 8 in. The six counters in the outer ring were connected in parallel to form set $B$. The center counter, labelled $A$, was separate. The data registered consisted of coincidences $AB$ and anticoincidences $A$–$B$. The

* Present address: National Bureau of Standards, Washington, D. C.

[1] G. J. Perlow and C. W. Kissinger, Phys. Rev. **81**, 552 (1951).

[2] T. R. Burnight, Phys. Rev. **76**, 165(A) (1949) has described rocket measurements of soft x-rays above the atmosphere. The intensity was enough to visibly blacken a photographic plate behind a very thin aluminum window in a few minutes. It appears reasonably clear however, that this phenomenon has an origin different from that of cosmic radiation. See also: Tousey, Watanabe, and Purcell, Phys. Rev. **83**, 792 (1951), and Friedman, Lichtman, and Byram, Phys. Rev. **83**, 1025 (1951).

[3] T. A. Bergstralh and C. A. Schroeder, Phys. Rev. **81**, 244 (1951).

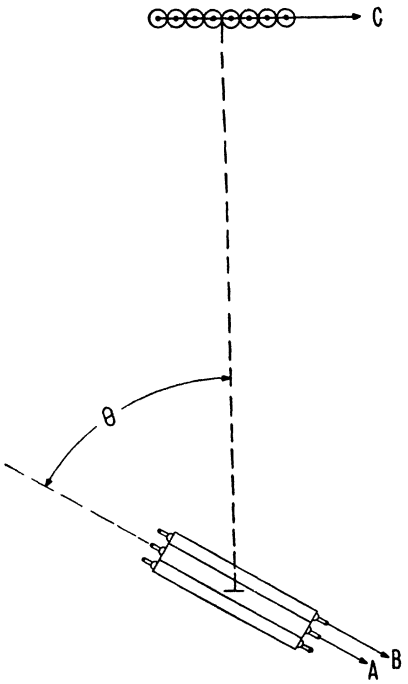


FIG. 2. Measurement of leakage. By taking data at various angles $\theta$ to the vertical, the inefficiency of the $B$ ring may be calculated for isotropic radiation.

former events were due to ionizing particles traversing counter $A$ and tripping one or more counters of the surrounding ring $B$. The anticoincidences $A$–$B$ represented the effect of a radiation which produced ionizing particles in the walls immediately surrounding the active volume of $A$, which particles, however, were not sufficiently energetic to penetrate the walls a second time and trip a $B$ counter. $AB$ thus measures charged particles, energetic $\gamma$-rays, and energetic neutrons, but is very much more effective for the charged particles. $A$–$B$ measures low energy $\gamma$-rays and low energy neutron-produced radiation. It is much more effective for the $\gamma$-rays, however.

The energy range of $\gamma$-rays which will produce anticoincidences $A$–$B$ is determined at the lower limit by absorption in the walls and at the upper by the energy of the secondaries. For the lower limit we may conveniently take an energy such that the intensity is reduced by a factor $1/e$ at the inner wall of counter $A$. This corresponds to a $\gamma$-ray energy of 100 kev. The upper limit is considerably less sharp because there is no minimum energy transfer which may occur in a Compton collision. The matter is discussed under "efficiency" in Sec. III.

There were two causes of error inherent in the apparatus which permitted some ionizing rays to count as anticoincidences. In both cases corrections could be applied. One was the lack of perfect shielding efficiency of the $B$ ring for ionizing radiation which penetrated counter $A$. This was measured by the arrangement shown in Fig. 2. A bank of counters $C$ was placed above the bundle and the rates $N_{AC-B}$ and $N_{AC}$ measured as a function of angle $\theta$. The inefficiency $\eta$ (=1-efficiency) in an isotropic field of radiation is given by

$$\eta=\int_0^{\pi/2} N_{AC-B}(\theta)\sin\theta d\theta \Big/ \int_0^{\pi/2} N_{AC}(\theta)\sin\theta d\theta.$$

The integrations were done graphically using measured values of the rates. For the various bundles used $\eta$ was 2.3–2.5 percent. The dependence of the ratio $N_{AC-B}/N_{AC}$ on $\theta$ showed that all but a negligible part of the inefficiency at sea level counting rate was geometrical in origin.

A second cause of error was double-pulsing in the $A$ counter. That is, a certain fraction of the $A$ counts are followed by a spurious discharge in a time less than $\sim 10^{-3}$ sec. The latter register as an event $A$–$B$. It is known that spurious pulses of this type are associated with the plateau slope in a Geiger counter. For this reason all the counters chosen had usable plateaus of at least 500 volts (threshold = 1000v) and plateau slopes of less than 0.04 percent/volt at 1220 v, the flight value. The circuit used to test the counters had a recovery time ($\sim$25 $\mu$sec) sufficiently short to be sensitive to double pulsing. In addition, a direct measurement of double pulsing was made by stretching to 4200 $\mu$sec the output pulse which signaled a coincidence $AB$, and placing this in turn in coincidence with the output pulse from the $A$–$B$ circuit. The latter had a width of 5 $\mu$sec. The effect is shown as a function of counter voltage for two typical bundles in Fig. 3. After subtraction of the predicted accidental rate, the effect re-

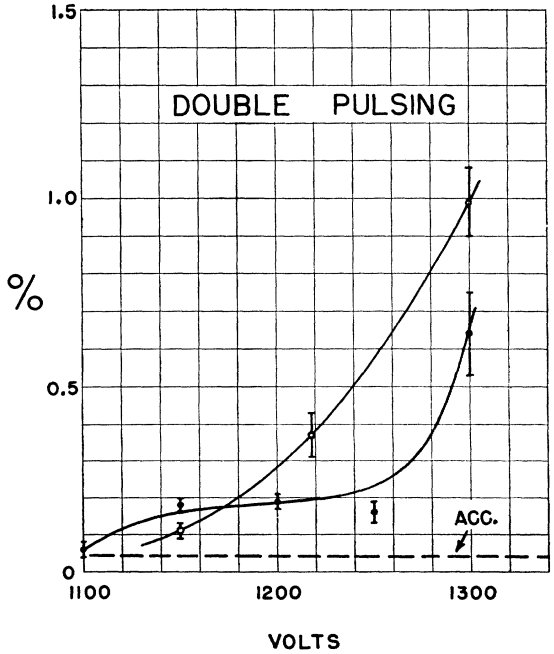


FIG. 3. The ordinate gives the relative number of times that counter $A$ was followed by a spurious pulse.

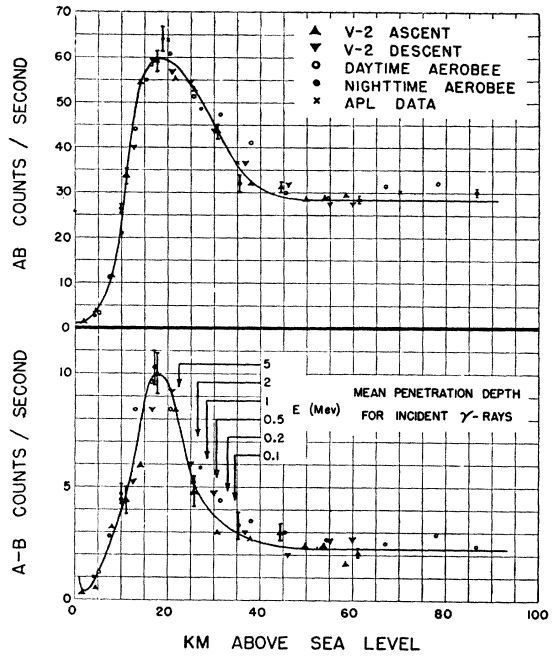


FIG. 4. Data of three flights.

maining was about 0.3 percent of the $AB$ rate at 1220 volts.

In all cases the bundle was mounted in the nose of the rocket and the surrounding material kept to a minimum. The rocket skin thickness was 0.125-in. Al for the V-2 and 0.050-in. Al for the Aerobee. The bundle and the rocket were co-axial. All counters were of the ether-argon type, manufactured commercially in a single batch, and all those tested a year after purchase had maintained their original threshold voltages and plateau slopes. Diode coincidence circuits were employed in the electronics.[4]

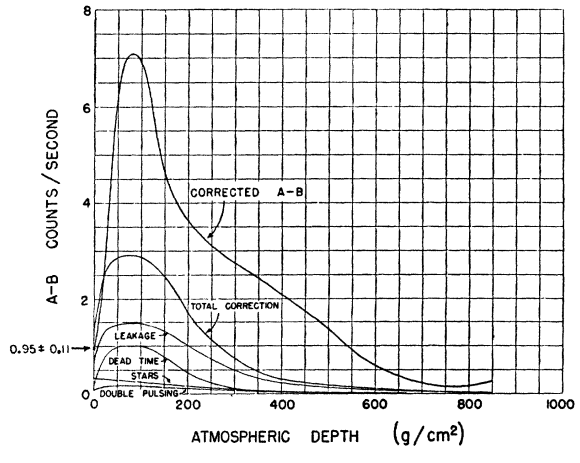


FIG. 5. Corrections and corrected anticoincidence rate obtained from smooth curve of Fig. 4.

[4] Howland, Schroeder, and Shipman, Jr., Rev. Sci. Instr. **18**, 551 (1947).

Figure 4 shows the data of the three flights plotted against altitude. Points are included for the ascending and descending legs down to where the rocket nose was blown off to facilitate recovery of other equipment.[5] The instrument space lost pressure during the night flight, resulting in electrical arc-over so that data were not obtained above 37 km. However, this was sufficiently high to observe that no measured diurnal effect existed in either the ionizing or the $\gamma$-radiation. In Fig. 4 we have indicated the depth of penetration for vertical incoming $\gamma$-rays of various energies to which the bundle can respond. The penetration considered is the mean free path to the first Compton collision. Vertical radiation will penetrate further due to successive collisions. The measurements of Bergstralh and Schroeder[2] confirm the absence of a diurnal effect within the much better statistical accuracy obtainable in a long balloon flight.

The orientation in space of all rockets varied during flight. The agreement between ascent and descent shows the indifference of the bundle to orientation. For the $AB$ curve, points are shown from the composite curve of single counter data reported by the APL group.[6] Their counting rates have been normalized to ours by multiplication by 8/6, the ratio of the nominal active lengths of the counters. The agreement is seen to be good. The increase in the $A-B$ counting rate at very low altitudes is a real effect due to ground radioactivity.

Figure 5 has been obtained from Fig. 4 by correcting the smooth curve and replotting against atmospheric depth. The corrections and the corrected curve are shown. In addition to the shielding and double pulsing effects discussed before, there is a correction for electronic and counter dead-time and one for neutron-induced stars. For the latter we have proceeded in much the same way as in the previous paper.[1] The starting point is the emulsion measurement of Yagoda *et al.* made in a V-2 and their observation that the prong distribution is characteristic of the stars produced by secondaries. The mountain altitude data of the Bristol group[7] is used to obtain the distributions. The stars which affect the $A-B$ rate are of type "0$n$" with no "grey" prongs, since the range of the latter is adequate to produce an $AB$. The probability $P$ of a star-generated event is taken as

$$P=Q\sum_N C_N D_N \exp\{-g(N)\}.$$

Here $Q$ is the probability that a star is produced within the range of a 10-Mev proton (typical "black" track) from the active volume of counter $A$. $C_N$ is the probability that the star contains $N$ prongs (grey or black). $D_N$ is the probability that one of the black particles enters the active volume. It is greater than 0.9 for $N>3$. The factor $\exp\{-g(N)\}$ is the probability (based

[5] G. J. Perlow, Sci. Monthly **69**, 382 (1949).
[6] Gangnes, Jenkins, Jr., and Van Allen, Phys. Rev. **75**, 57 (1949).
[7] Brown, Camerini, Fowler, Heitler, King, and Powell, Phil. Mag. **40**, 862 (1949).

on a poisson distribution) that an $N$ prong star with an expected number of grey tracks $g(N)$ actually contains none. The variation of $P$ with height is contained in $Q$. We have used the data of Lord[8] for the slope of the variation and of Yagoda and others[9] for normalization to the free-space point. The star correction amounts to 15 percent above the atmosphere and is unimportant at depths greater than 40 g/cm². It is probably overestimated at all depths.

Table I is a summary of the data above the atmosphere. The V-2 data cover the region 51 to 60 km, or 90 seconds, and the daytime Aerobee 46 to 80 km, or 50 seconds. The choice of altitude ranges is governed by such factors as absence of noise on the telemetering record, uprightness of the rocket, etc. There is a small difference between the counting rates in the two rockets. Skin thickness, difference in dimension, and true intensity difference probably all enter in. The difference in $A-B$ rates after correction is just outside of statistical probable error.

In order to get some idea of the energy above the atmosphere despite our ignorance of its spectral distribution, we assume for the moment that all we measure are photons below ~7 Mev. For these, the efficiency is approximately proportional to energy and we may assign an energy flux without knowledge of the spectrum, as in reference 1. In this way we obtain ~0.3 Mev/cm² sec sterad for the unidirectional energy intensity and ~0.9 Mev/cm² sec for the flow across 1 horizontal cm². This is seen to be comparable to the quantity reported in reference 1 for the energy range $3.4 \leq E \leq 90$ Mev and ~2000 times smaller than the total incoming energy which goes into atmospheric ionization.

We have applied the pertinent (and small) corrections to obtain a corrected $AB$ rate and a value of the unidirectional charged particle intensity assuming isotropic radiation from the upper hemisphere. This result is in agreement with the single counter measurements of the APL group.[6] The vertical intensity at this latitude is considerably lower[10] than the figure so obtained. The difference is presumably due to albedo, i.e. to secondaries from the atmosphere.

## III. THE ATMOSPHERIC RADIATION

### A. Calculation of the Spectrum

We may note first that the atmospheric gamma-radiation is quite intense. At the intensity maximum its counting rate is about one-tenth that of the ionizing radiation, but the detection efficiency for much of it is only a few tenths of one percent. Thus its intensity is in the order of 100 times greater than that of the charged particles. This factor may be understood by an analysis of the origin of the radiation.

TABLE I. The radiation above the atmosphere.

| | V-2 | Aerobee |
|---|---|---|
| $AB$ | 28.3±0.4 | 30.6±0.5/sec |
| $A-B$ | 2.3±0.1 | 2.7±0.2 |
| Corrections to $A-B$ | | |
| Leakage | 0.71 | 0.77 |
| Double-pulsing | 0.07 | 0.08 |
| Dead-time | 0.21 | 0.25 |
| Stars | 0.33 | 0.33 |
| Total corrections | 1.3 | 1.4 |
| Corrected $A-B$ | 1.0±0.1 | 1.3±0.2 |
| "Vertical" $\gamma$-ray energy flow | 0.3 Mev/cm² sec sterad | |
| $\gamma$-ray enery flow across 1 horizontal cm² assumed to come from one hemisphere | 0.9 Mev/cm² sec | |
| Corresponding quantity from previous measurement, $3.4 \leq E \leq 90$ Mev | 1.4 Mev/cm² sec | |
| Total primary energy flow (Millikan *et al.*) | 1800 Mev/cm² sec | |
| Corrected $AB$ (V-2) | 29.2±0.4/sec | |
| Charged particle intensity (hemispherical isotropy assumed) | 0.12/cm² sec sterad | |
| APL single counter[a] | 0.13/cm² sec sterad | |

[a] See reference 6.

We expect the following sources of the low energy gamma-rays: 1. The bremsstrahlung of electrons. 2. The annihilation of positrons. 3. The direct production of low energy quanta by neutral meson decay. In addition there is present the secondary radiation arising from multiple Compton scattering of these three. Further sources which may contribute to a small extent are nuclear gamma-rays and the x-rays associated with capture of negative mesons into atomic orbits. These are not treated.

We have calculated the effect of item 1 in some detail and have made estimates of items 2 and 3. Considering the last item, the Bristol group[11] has obtained $\gamma$-ray

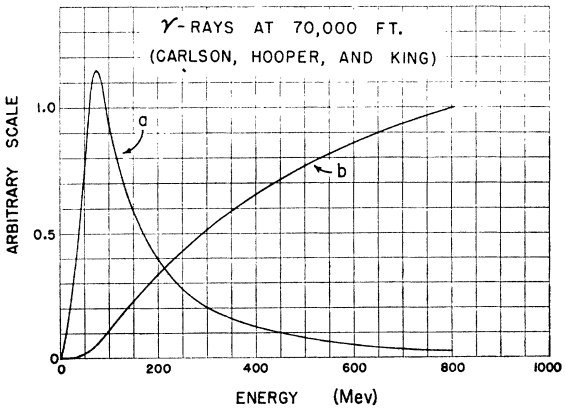


FIG. 6. Intensity of $\gamma$-rays from $\pi^0$ meson decay. Curve a, differential number spectrum $n(E)$. Curve b, integral energy spectrum $\int_0^E En(E)dE$.

[8] J. J. Lord, Phys. Rev. **81**, 901 (1951).
[9] Yagoda, de Carvalho, and Kaplan, Phys. Rev. **78**, 765 (1950).
[10] J. A. Van Allen and S. F. Singer, Phys. Rev. **78**, 819 (1950). Winkler, Stix, Dwight, and Sabin, Phys. Rev. **79**, 656 (1950). Perlow, Bergstralh, Johnson, and Shipman, Jr., Phys. Rev. **80**, 133(A) (1950).
[11] Carlson, Hooper, and King, Phil. Mag. **41**, 701 (1950).

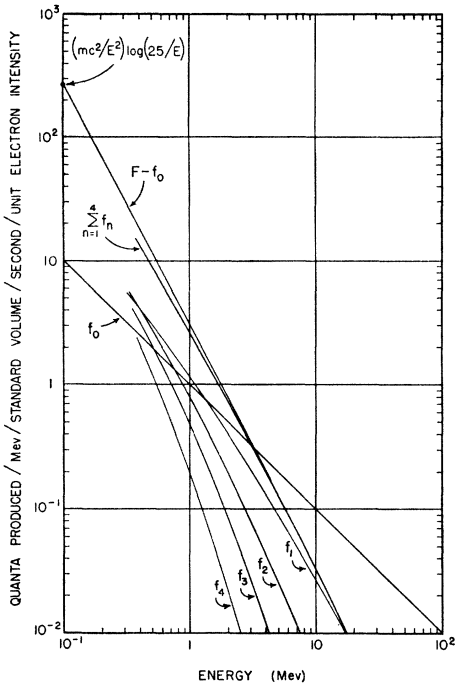


FIG. 7. Production spectrum of the various components of the $\gamma$-radiation. $f_0$ is the parent bremsstrahlung spectrum; $f_1 \cdots f_4$ the successive generations of scattering. $\Sigma f_n$ is the sum of 4 scattered generations; $F-f_0$ is the complete scattering spectrum determined by joining $\Sigma f_n$ to the indicated point at 0.1 Mev.

spectra at 70,000 ft altitude which they show to be due to $\pi^0$ decay. Their differential number distribution $n(E)$ is shown in Fig. 6 as curve a. Curve b is a plot of $\int_0^E En(E)dE$ the energy contributed by all photons having quantum energy $<E$. The great preponderance ($>90$ percent) of the energy originates as energetic quanta ($E>100$ Mev) which therefore produce the electronic cascades and item 1. We are thus justified in neglecting item 3.

The calculation of item 1 proceeds from the following: the electron cascades are maintained by the complementary processes of bremsstrahlung and pair production. The spectrum radiated by an electron, to a conventional approximation, is independent of the latter's energy, and as regards number of quanta, the lower quantum energies are favored as $1/E$. Sometimes a photon suffers a Compton collision and thereby escapes the cascade, since its energy is then usually reduced to the point that a second such collision is more probable than the production of a pair. Successive Compton effects then follow, leading finally to low energy and photoelectric absorption. The recoil electrons may be energetic enough in the early stages of the process to form part of the radiating population which exists in the equilibrium situation. Since we are interested only in the ratio of photons to electrons, the origin of the latter is of no concern. In the median case an electron requires an energy of $\sim 7.5$ Mev to be observed by the bundle, while $\gamma$-rays of $<15$ Mev may count. Electrons of energy between these values are a special case. However, we shall assume them to radiate the same spectrum as those above 15 Mev. We also assume that those below 7.5 Mev do not radiate at all. The errors in these assumptions are compensatory and small in any case.

The $\gamma$-ray intensity depends on values of the electron intensity within distances of a few mean free paths from the point of measurement. If the electron intensity is uniform over this region, the details of the cascade are irrelevant and the calculation becomes much simpler.[12] This is the case we treat. It should be correct at the intensity maximum, while giving too high an intensity of $\gamma$-rays above this altitude and too low below.

The electron intensity is assumed to be isotropic over a sphere as a computational convenience. Isotropy over a hemisphere gives the same results, and even large deviations from isotropy have only a slight effect since the bundle is not very sensitive to orientation.

We calculate below the production spectrum of bremsstrahlung, the production spectrum of the scattered radiation, from these the intensities, and by means of an efficiency factor relate the latter to the counting rates of electrons and $\gamma$-rays.

An intensity of 1 electron/cm$^2$ sec sterad corresponds to a total length of track $4\pi$ cm/sec in one cm$^3$ of volume. In the approximation we use there are $dE/E$ photons of energy $E$, $dE$ radiated per radiation length ($X_0$ cm) of path. Hence, if we choose as a standard, a volume of numerical magnitude $X_0/4\pi$ cm$^3$, the differential production spectrum of bremsstrahlung may be written:

$$f_0(E)dE=dE/E, \tag{1}$$

where $f_0(E)dE$ is the number of quanta of energy $E$, $dE$ produced per standard volume per second by unit electron intensity.

The production spectrum of scattered radiation may be calculated by taking $f_0(E)$ as the progenitor of a next generation $f_1(E)$. In similar fashion $f_1(E)$ produces a next generation $f_2(E)$ and so on.

$$\begin{aligned} f_1(E)dE&=dE\int_E^\infty f_0(E')P(E', E)dE', \\ &\vdots \\ f_n(E)dE&=dE\int_E^\infty f_{n-1}(E')P(E', E)dE' \end{aligned} \tag{2}$$

where $P(E', E)dE$ is the probability that a photon of energy $E'$ will produce one of $E$ in $dE$ by means of a Compton collision. The complete production spectrum

[12] The closely allied problem of the radiation intensity in a medium containing a uniformly distributed radioactive source has been treated by W. R. Faust and M. H. Johnson, Phys. Rev. **75**, 467 (1949) and by P. R. Karr and J. C. Lamkin, Phys. Rev. **76**, 1843 (1949). Our treatment of the scattering is somewhat similar to the latter.

is the sum:

$$F(E)dE=dE\sum_{n=0}^{\infty}f_n(E). \tag{3}$$

$P(E', E)$ takes into account that the photon $E'$ may produce a pair instead of scattering, thus:

$$P(E', E)=\{Z\varphi_c(E')/[Z\varphi_c(E')+\varphi_{pr}(E')]\}\cdot d\varphi_c(E', E)/\varphi_c(E'). \tag{4}$$

where $\varphi_c$ and $\varphi_{pr}$ are the total cross sections for Compton effect and pair production per electron and atom respectively.[13] The quantity $d\varphi_c$ is the differential Klein-Nishina cross section and may be written:

$$d\varphi_C(E', E)=\frac{\pi e^4}{mc^2}\cdot\frac{1}{E'^2}\left[\frac{E'}{E}+\frac{E}{E'}-1+\left\{\frac{mc^2}{E'}-\frac{mc^2}{E}+1\right\}^2\right]dE \tag{5}$$

whenever $E'\geq E\geq E'/(1+2E'/mc^2)$ from the Compton formula. Otherwise $d\varphi_c=0$.

Mr. H. Caulk has evaluated $F(E)$ to $n=4$ by numerical means. The infinite upper limit of Eq. (2) was replaced by 100 Mev. For the region below $\sim mc^2$, the convergence is no longer rapid and a separate treatment is required. Asymptotically the mean wavelength change in scattering approaches the Compton wavelength $\lambda_0\equiv h/mc$ for $\lambda\gg\lambda_0$. After many scatterings, the quanta "forget" their remote ancestry and we may write for the number of low energy quanta produced by one ancestor:

$$q(\lambda)d\lambda=d\lambda/\lambda_0 \tag{6}$$

independent of the original energy, or

$$q(E)dE=mc^2dE/E^2,\quad E\ll mc^2, \tag{7}$$

whence

$$F-f_0\rightarrow q(E)\int_0^{E_u}f_0(E')dE'. \tag{8}$$

Pair production is taken care of in the choice of $E_u$. For $E>E_u$ materialization is assumed invariably, while $E<E_u$ produces scattering only. A simple numerical calculation using the total cross sections for pair production and Compton scattering gives $E_u\sim 25$ Mev. The result is not very sensitive to this value. Inserting (1) and (7) in (8) and integrating, we obtain

$$F(E)-f_0(E)=(mc^2/E^2)\log(25/E),\quad E\ll mc^2. \tag{9}$$

This joins well with the values obtained above $mc^2$.

Figure 7 is a graph of the various spectra. The $F-f_0$ curve is made to go through the point given by Eq. (9) at $E=0.1$ Mev.

The spectrum of scattered radiation is fitted quite well by

$$F(E)-f_0(E)=3.0E^{-2.0} \tag{10}$$

over the range $0.1\leq E\leq 15$ Mev. Therefore,

$$F(E)=1/E+3/E^2. \tag{11}$$

The simplicity of the final result is fortuitous. The intensity spectrum $I_\gamma(E)$ of the $\gamma$-radiation is related to the production spectrum by

$$I_\gamma(E)=I_eF(E)/\mu(E)X_0\ (\text{Mev cm}^2\ \text{sec sterad})^{-1}. \tag{12}$$

$I_e$ is the electron intensity, and $\mu(E)$ is the linear absorption coefficient. Introducing the air density $\rho$, the mass absorption coefficient $\mu/\rho$, and the radiation thickness $\rho X_0=43$ g/cm$^2$, we have

$$\frac{I_\gamma}{I_e}=\frac{1}{43\mu(E)/\rho}\cdot\left\{\frac{1}{E}+\frac{3}{E^2}\right\}. \tag{13}$$

$I_\gamma/I_e$ is plotted *vs* $E$ in Fig. 8.

### B. The Efficiency

A considerable literature[14] exists on the efficiency of a single Geiger counter for $\gamma$-radiation incident normal to the axis ("broadside" radiation). Our problem differs in three respects: a. The radiation is isotropic rather than broadside. b. The efficiency decreases above a certain energy due to penetration of the outer ring $B$ by conversion products. c. The disposition of material about the counting volume is more complicated. We define an efficiency function $B(E)$ for isotropic radiation. If $N_\gamma$ is the $\gamma$-ray counting rate of the device,

$$N_\gamma=\int_E B(E)I_\gamma(E)dE. \tag{14}$$

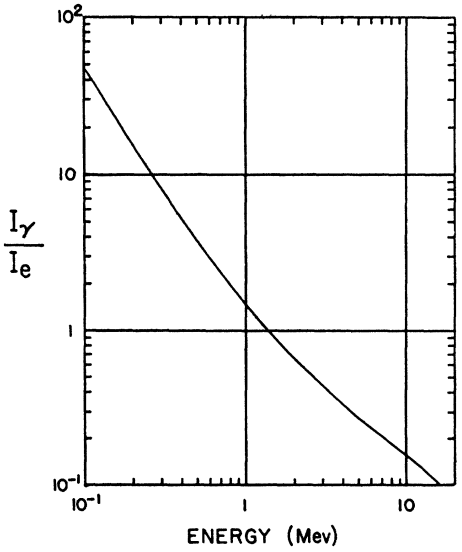


FIG. 8. Calculated relative intensity of $\gamma$-rays to electrons as a function of the $\gamma$-ray energy. The electrons have energy $>\sim 10^7$ ev.

[13] Values of the quantities appearing in this section have been taken wherever possible from W. Heitler, *The Quantum Theory of Radiation* (Oxford University Press, London, 1944), second edition.

[14] A bibliography may be found in M. Healea, Nucleonics **1**, 68 (1947).

The function $B(E)$ has been determined at $E=1.2$ Mev by use of a standard $Co^{60}$ source having a strength of 10 rutherfords ($2\times10^7\gamma$'s/sec).[15] The counting rate was determined as a function of the angle $\theta$ between the bundle axis and the line of length $R$ joining bundle and source. It may be shown that:

$$B(1.2)=(8\pi^2R^2/2\times10^7)\int_0^{\pi} N_\gamma \sin\theta d\theta. \quad (15)$$

We assume that $B$ varies with energy in the same manner as does the efficiency for broadside radiation. The data for copper counters of Renard[16] and the calculations of Marty[17] are used for the energy dependence and our value at 1.2 Mev for normalization. This applies up to an energy $E_p$ at which the secondaries can begin

TABLE II. Values of the quantities used in calculating the atmospheric radiation.

| $E$(Mev) | $B(E)$ | $\mu(E)/\rho$ | $\int_{\Delta E}\frac{B(E)}{E\mu(E)/\rho}dE$ | $\int_{\Delta E}\frac{3B(E)}{E^2\mu(E)/\rho}dE$ |
|---|---|---|---|---|
| 0.1 | 1.14 | 0.15 | | |
| | | | 3 | 82 |
| 0.15 | 0.89 | 0.13 | | |
| | | | 2 | 36 |
| 0.2 | 0.84 | 0.12 | | |
| | | | 3 | 41 |
| 0.3 | 1.04 | 0.11 | | |
| | | | 7 | 52 |
| 0.5 | 1.58 | 0.087 | | |
| | | | 22 | 90 |
| 1.0 | 3.21 | 0.063 | | |
| | | | 62 | 122 |
| 2.0 | 6.4 | 0.044 | | |
| | | | 82 | 100 |
| 3.0 | 9.9 | 0.036 | | |
| | | | 213 | 165 |
| 5.0 | 16.6 | 0.028 | | |
| | | | 292 | 146 |
| 7.2 | 24.3 | 0.023 | | |
| | | | 311 | 117 |
| 10.0 | 15.5 | 0.020 | | |
| | | | 194 | 58 |
| 15.0 | 0.0 | 0.0176 | | |
| Sum | | | 1191 | 1009 |

to produce coincidences. At this stage the geometry complicates the problem. We have simplified it as follows. The distribution in path length through the copper wall bounding the active volume of counter $A$ was determined by drawing-board techniques. The median thickness was determined from the distribution. The complex geometry was next considered as being replaced by a plane-parallel geometry with this wall thickness. $E_p$ was determined as the energy of the gamma-ray, whose secondaries had a mean energy just adequate to penetrate this wall. This corresponds to an electron energy[18] of 4.7 Mev and a $\gamma$-ray energy of 7.2 Mev. As the $\gamma$-ray energy is increased, there is less and less wall available for the conversion, and the efficiency decreases nearly linearly until the electron range is 2 wall thicknesses. At this point the efficiency vanishes. This occurs at an electron energy of 10.8 Mev corresponding to $\gamma$-rays of 15 Mev.

This picture is necessarily rough. We do not think it introduces too large an uncertainty into the results however. The counting rate contributed by $\gamma$-rays in the region of decreasing efficiency is calculated to be $\sim$30 percent of the total.

The counting rate of electrons is given by

$$\begin{aligned} N_e&=\pi I_e\times\text{surface area}\\ &=480I_e/\text{sec}. \end{aligned} \quad (16)$$

Using this, and Eqs. (13) and (14), we have

$$\frac{N_\gamma}{N_e}=\frac{1}{480\times43}\int_{0.1}^{15}\frac{B(E)}{\mu(E)/\rho}\left\{\frac{1}{E}+\frac{3}{E^2}\right\}dE. \quad (17)$$

Values of the various quantities are given in Table II. We have, finally,

$$N_\gamma/N_e=0.11. \quad (18)$$

The ratio of measured (and corrected) counting rates in the neighborhood of the intensity maximum is given by

$$N_{A-B}/N_{AB}=0.12. \quad (19)$$

We do not know exactly how much of $N_{AB}$ to ascribe to electrons and how much to other charged components. We may make an estimate based on Rossi's analysis[19] at the maximum for vertical radiation. He obtains $\sim$65 percent for the fraction of electrons of $>10^7$ ev to the total charged vertical component. If we assume this ratio at our maximum (radiation from all directions), we obtain

$$N_{A-B}/(N_{AB})_{\text{electrons}}\sim0.18. \quad (20)$$

Our calculation accounts for $\sim$60 percent of the measurement. The annihilation radiation of positrons is estimated below.

### *Annihilation of Positrons*

We require the number of positrons which annihilate per unit time in a given volume. An upper limit to the intensity $I_+$ of positrons is $I_+\sim I_e/2$, neglecting collision electrons and Compton recoils, and the path length traversed per cm$^3$ and second is $4\pi I_+$.

Dividing this by the average range of the atmospheric positrons gives the number of stopping per cm$^3$ and second. We may estimate the range as the radiation length $X_0$. Thus, for example, Heitler[20] gives the mean range of a 50-Mev electron as $\sim X_0/2$ and a 500-Mev electron as $\sim 2X_0$, the range increasing only logarith-

[15] We are indebted to the National Bureau of Standards for this source and its standardization.
[16] G. Renard, J. phys. et radium **9**, 212 (1948).
[17] N. Marty, J. phys. et radium **8**, 29 (1947).
[18] F. L. Hereford and C. P. Swann, Phys. Rev. **78**, 727 (1950).
[19] B. Rossi, Revs. Modern Phys. **20**, 537 (1948).
[20] See reference 11, p. 223.

mically with energy. Then in the standard volume ($X_0/4\pi$ cm$^3$) we have for $I_e=1$, as production spectrum of parent quanta,

$$f_{0+}(E)=\delta(E-mc^2) \tag{1'}$$

for this energy region Eq. (7) is a reasonable approximation for the scattered spectrum. The calculation then procedes analogously,

$$F_+(E)=mc^2/E^2+\delta(E-mc^2), \tag{11'}$$

$$I_{\gamma+}(E)=F_+(E)I_e/\mu(E)X_0 \tag{12' and 13'}$$

$$=\frac{I_e}{43\mu(E)/\rho}\left\{\frac{mc^2}{E^2}+\delta(E-mc^2)\right\},$$

$$N_{\gamma+}/N_e=\frac{1}{480\times 43}\left\{\int_{0.1}^{0.51}\frac{mc^2}{E^2}\frac{B(E)}{\mu(E)/\rho}dE+\frac{B(mc^2)}{\mu(mc^2)/\rho}\right\}. \tag{17'}$$

The integral, which represents the effect of scattering, is evaluated from the data in Table II as before. It has the value 36, compared to 18 for the second term which represents the annihilation quanta. Then

$$N_{\gamma+}/N_e=0.0026. \tag{18'}$$

This is negligible compared to the bremsstrahlung, (Eq. (18)).

We may conclude this section with the observation that, all approximations considered, the explanation given of the sources of the atmospheric radiation accounts for the measurements and that there is not room for any important additional source.

## IV. THE RADIATION ABOVE THE ATMOSPHERE

After all corrections, the $\gamma$-ray counting rate per second above the atmosphere (Table I) remains at $1.0\pm0.1$ for the V-2 and $1.3\pm0.2$ for the daytime Aerobee. The probable errors shown are the statistical ones. The difference between the two flights may be taken, if one chooses, as due to an unknown systematic correction rather than a true effect. We have no choice, however, but to acknowledge the existence of a gamma-ray flux above the atmosphere. For the Aerobee flight it is possible to ascertain whether there was any significant change in counting rate above 50 km. None was observed. We do not believe however that the radiation is primary. Some, if not all, of it certainly originates in the atmosphere below the rocket and escapes out. We shall show below how a part of this has been calculated.

We consider two cases. In the first the earth is assumed flat and the radiation leaving the atmosphere is due to diffusion upward. A calculation of this is similar to that of determining the back scattering of $\gamma$-rays incident on an absorber[21] but is made more difficult by the fact that the $\gamma$-rays themselves are secondaries and are produced at various depths in the absorber. We have attempted a rough solution of the problem by analogy to the random walk, but we have not obtained a trustworthy result other than that the phenomenon exists and must produce some "albedo."

The second case depends on the curvature of the earth and is amenable to calculation. Primaries at grazing incidence, whose extended paths would reemerge from the atmosphere, produce low energy $\gamma$-rays by intermediate processes. These leave the atmosphere and form part of the albedo. Although the solid angle subtended at the rocket for such an effect is small, the multiplication along the relatively long air paths makes it significant. Figure 9 shows the process. The rocket is at height $h$. A primary ray under consideration has a path which passes a perpendicular height $p$ from the earth. According to the rocket measurements of R. Havens,[22] the atmospheric thickness above $p$ is given by $t_p=a\exp(-h/H)$, where the "scale height" $H$ has the value 8.2 km and $a=420$ g/cm$^2$. This holds within seasonal variation at $p=40$–$60$ km where the effect

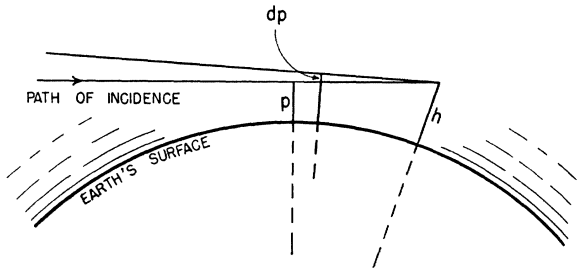


FIG. 9. Production of $\gamma$-ray albedo due to curvature of the earth.

mainly occurs. The atmospheric thickness $t_i$ traversed along the path of incidence has a nearly constant proportionality $t_i=63t_p$ in this same range, according to calculations of Newell and Pressly[22] based on Havens' atmosphere.

We have to consider the spread of the radiation about the direction of incidence. Examination of the calculation of the previous section shows that the counting rate would be diminished by only 15 percent if the detector responded only to energies above 1 Mev. For such energies the angular spread is relatively small. If it is taken as zero and calculation made for various $h$, and if the result does not vary much with $h$, we shall be justified in assuming that the scattering of rays away from the direction of incidence is approximately balanced by the scattering of others toward it. A trial calculation shows this to be the case. We have therefore neglected the angular spread.

In order to obtain the $\gamma$-ray intensity along the path

[21] L. L. Foldy, Phys. Rev. **82**, 927 (1951). L. V. Spencer and F. Jenkins, Phys. Rev. **76**, 1885 (1949).

[22] Private communication.

of incidence, a Gross transformation has been made of the corrected altitude counting rate curve. This gives approximately the vertical intensity in units of $\gamma$-ray counts/sec sterad per bundle. By virtue of the isotropy of the primaries, the intensity along the path of incidence has the same variation with thickness traversed. The intensity and composition of the primary radiation need not be considered. The transformed function may be approximated, for our purpose, by straight lines:

$$I(t_i)=\begin{cases} t_i/60, & 0\leq t_i\leq 130 \text{ g/cm}^2 \\ 4.3-t_i/60, & 130\leq t_i\leq 220 \text{ g/cm}^2. \end{cases} \quad (21)$$

The calculation is not taken to greater thickness. The greatest vertical depth considered is $t_p=3.5$ g/cm$^2$ corresponding to 39.3 km. The lines intersect at $p=43.6$ km. With the aid of a little geometry we may show that the counting rate of albedo is $N=N_1+N_2$, where approximately

$$\begin{aligned} N_1&=K_1\int_{43.6}^{h}(h-p)^{-\frac{1}{2}}\exp(-p/H)dp, \\ N_2&=K_2\int_{39.3}^{43.6}(h-p)^{-\frac{1}{2}}dp \\ &\quad -K_1\int_{39.3}^{43.6}(h-p)^{-\frac{1}{2}}\exp(-p/H)dp, \\ K_1&=2\pi 63a/60(2R_e)^{\frac{1}{2}}, \quad K_2=2\pi 4.3/(2R_e)^{\frac{1}{2}}, \end{aligned} \quad (22)$$

and $R_e$ is the earth's radius. The integral in $N_1$ can be transformed into a form evaluable from tables[23] of $\int\exp(x^2)dx$. For $h=82$ km we obtain $N_1=0.17$, $N_2=0.07$, whence $N=0.24$ count/sec.

This is one-fourth of the corrected rate above the atmosphere. It is likely that the remaining three-fourths would be explained by a treatment of the "flat-earth" or diffusion albedo.

It should be noted that a similar treatment may be accorded the various other secondary radiations. One expects, for example, an albedo of electrons, protons, and neutrons. Calculation of the former two is complicated by the earth's magnetic field.

If the albedo explanation of the observed flux is correct, then our measurements taken along with those at high energy indicate at most a very small primary gamma-ray component. An immediate implication is support for the contention that magnetic fields exist over large regions of space. As is well known, the fields increase the path length, hence the intensity, of charged particles and not that of photons.

The authors are grateful for the continued interest and encouragement of Dr. H. E. Newell, Jr., in their work. We wish to acknowledge the aid of other colleagues in the Rocket Sonde Branch, chiefly; Mr. H. M. Caulk for numerical evaluation of the scattering integrals; Messrs. J. Siry and H. Spitz and Miss E. Pressly for other mathematical work at various times; Messrs. J. T. Mengel, D. Mazur, and N. R. Best for telemetering of data from the rockets; Mr. C. P. Smith, Mr. V. Goblirsch, and the late Mr. R. Chamberlain for the engineering details associated with the rocket installations. Mr. C. A. Schroeder helped in the electronic design and Mr. P. R. McCray in the construction. In addition we are grateful for help in telemetering from the personnel of the New Mexico College of Agriculture and Mechanical Arts, chiefly Messrs. C. Ricketts and H. A. Ware. We were aided by military and civilian personnel of the White Sands Proving Ground and wish especially to thank Maj. N. Pozinsky, USMC, Mr. H. Karsch and Mr. L. D. White.

We have had fruitful conversations during the course of this investigation with Dr. M. H. Johnson and Professor J. A. Wheeler.

[23] H. M. Terrill and L. Sweeney, J. Franklin Inst. **237**, 495 (1944).